J Mater Sci (2019) 54:10548–10559

Polymers

Conduction through plasma-treated polyimide: analysis of high-field conduction by hopping and Schottky theory

Michael A. Vecchio[1,*], Amira Barhoumi Meddeb[2], Zoubeida Ounaies[3], and Michael T. Lanagan[4]

[1] *Materials Science and Engineering Department, Penn State University, N-326 Millennium Science Complex, University Park, PA 16802, USA*

[2] *Mechanical and Nuclear Engineering Department, Penn State University, N259 Millennium Science Complex, University Park, PA 16802, USA*

[3] *Mechanical and Nuclear Engineering Department, Penn State University, 157B Hammond Building, University Park, PA 16802, USA*

[4] *Engineering Science and Mechanics Department, Penn State University, N-329 Millennium Science Complex, University Park, PA 16802, USA*

Received: 30 November 2018
Accepted: 27 March 2019
Published online: 11 April 2019

ABSTRACT

Plasma surface modification of polyimide (PI) films has been used to modify the material's wetting and adhesion properties but has also been found to impact high-field electrical properties. Previous work by Meddeb et al. (Chem Phys Lett 649:111–114, 2016. https://doi.org/10.1016/j.cplett.2016.02.037) demonstrates a significant reduction in high-field leakage current at high temperatures because of O_2 plasma treatment of PI. In this study, we investigate field-dependent current density [$J(E)$] data measured in our previous study by Meddeb et al. (2016) to identify the surface and bulk mechanisms responsible for high-field conduction behavior of O_2 plasma-modified PI films. Specifically, we analyze the $J(E)$ data using three conduction theories: Poole–Frenkel, Schottky, and Hopping. Poole–Frenkel and Schottky analyses are performed by the implementation of linear regression. Hopping analysis was performed using a rigorous statistical technique that incorporates nonlinear regression as well as a bootstrap statistical analysis of fit parameters. Analysis of $J(E)$ data over the temperature range 25–175 °C indicates that 13-micron-thick untreated PI films are dominated by a hopping process at lower temperatures; however, transition to Schottky-dominated conduction occurs as temperature is increased. Films treated with O_2 plasma show similar characteristics to the untreated set: Hopping dominated conduction at low temperatures with gradual transition to Schottky. However, the transition to Schottky conduction occurs at a higher temperature in plasma-treated films in comparison with the untreated control

Address correspondence to E-mail: mav206@psu.edu

https://doi.org/10.1007/s10853-019-03574-w

set. These results are verified by (1) extracting dielectric permittivity from Schottky plots as a function of temperature and (2) a statistical interpretation of confidence intervals calculated for hopping fit parameters used in low-temperature nonlinear regression. Outcomes from theoretical analysis of the data are used to provide further insight into how surface chemistry may be tailored to limit high-field leakage current in polyimides and insulating polymers in general.

Introduction

There exists a need to develop next-generation materials for power electronic applications with lighter weights and smaller volumes, yet capable of operating with high efficiency at high temperatures. Organic dielectric materials are one option, due to their ease of manufacturability, light weight, and favorable electrical properties such as high breakdown strength. Currently, biaxially oriented polypropylene (BOPP) is considered the state of the art in capacitor films, exhibiting a breakdown strength on the order of 850 MV/m [1] and theoretical power densities calculated to be in the range of 10^8 W/cm^3 [2]. Other materials relevant to high-voltage dielectric applications are polar polymers such as polyvinylidene fluoride (PVDF) along with its associated copolymer poly(vinylidene fluoride–trifluoroethylene) (P(VDF–TrFE)) and terpolymer poly(vinylidene fluoride–trifluoroethylene–chlorotrifluoroethylene) (P(VDF–TrFE–CTFE)). Recent research done on blended PVDF/P(VDF–TrFE–CTFE) composites show impressive breakdown strengths (640 MV/m) and energy densities measured as high as $\sim$ 20 J/cm^3 [3, 4]. Routes to improve the high-field performance of pure organic dielectrics that depends on more involved processing procedures have also been studied. Past research done on organic dielectrics fabricated by the coextrusion of P(VDF–HFP) and polycarbonate (PC) demonstrates the ability of the composite material to achieve a breakdown strength that exceeds that of either constituent material [5].

Although these materials show promise to develop the class of next-generation power and energy-dense organic electronics, their low melting temperatures near 160 °C limits their ability to withstand energy dissipation attributed to high dielectric loss and leakage currents. This can be conceptualized by a device's performance represented by a Ragone plot: In the case of power electronics, the boundaries of capacitor performance are represented by power versus energy density and are determined by the material's internal losses and/or leakage [6]. In the case of PVDF, its polar nature causes the material to be inherently susceptible to high dielectric loss [7] exhibiting loss tangents that reach as high as $\sim$ 0.5–1.0% [8]. As a result, PVDF experiences high leakage currents at DC frequencies even at low temperatures, within the range of 10^{-3}–10^{-2} A/m^2 at fields exceeding 20 MV m^{-1} depending on material geometry and processing technique [8, 9]. In the case of nonpolar BOPP, dielectric absorption is very low, exhibiting dielectric loss tangents as low as 10^{-4} at low fields [10]. However, the application of high electric fields required for high-power and energy applications causes energy dissipation in the form of leakage current. This leads to Joule heating, a precursor to dielectric breakdown [11, 12], causing temperature elevation of the material regardless of ambient operating conditions, and bringing the material closer to its relatively low derating temperature of 80 °C [7].

Another influence which limits the applicability of these materials is ambient operating temperatures for applications that require thermal stability within the range of PVDF's and BOPP's melting temperatures. For example, passive electronics fabricated for automotive applications must retain continuous structural and electrical stability within 150–200 °C, measured on engine and in transmission during vehicle operation [13, 14]. This creates a demand for volumetrically efficient capacitors that can maintain high voltage/temperature stability manufactured at low costs. Unlike BOPP, PC, and PVDF blends and composites, polyimide (PI) exhibits a combination of large breakdown strength measured at 615 MV m^{-1} [15] and high glass transition temperatures reported in the range of 370–470 °C depending on chemical

structure and processing [16, 17]. Low dielectric dissipation factor in the range of 10^{-3} (provided by Dupont™ Kapton® HN material data sheet as well as literature [18]) and a potential of high energy and power density add to its appeal as a next-generation high-field dielectric material. Despite these favorable properties of PI, high-temperature environments combined with charge injection at the electrode/dielectric interface put the material at risk of Joule heating and high leakage currents during operation. Implementation of processing procedures that can limit the leakage current through PI at high temperatures are required to achieve its full potential as a high-temperature dielectric polymer.

Reactive plasma treatments of polymers have been shown to have a significant impact on material chemistry [15, 19, 20] and properties such as wettability [21, 22] and adhesion [23–26]. In addition, plasma treatment has been demonstrated to influence electrical properties. In previous work by Mammone et al. [27], plasma treatment processing using 96% CF_4/4% O_2 on polypropylene resin prior to melt extrusion was shown to increase the dielectric breakdown strength of the material by 20%. Similar work done that uses 96% CF_4/4% O_2 plasma treatment on the surface of 12-micron PVDF films led to 11% increase in dielectric breakdown strength relative to untreated control samples [28]. Recently, research done in our group by Meddeb et al. [15] showed that plasma surface treatment using pure O_2 on PI resulted in reduced spread in dielectric data, improved Weibull modulus at low temperatures and improved breakdown strength at elevated temperatures. Among these observations, an order of magnitude reduction in leakage current at 150 °C was also noted. This study provided a thorough chemical analysis using XPS and H_2O sessile drop experiments to characterize the surface of the films after plasma treatment and surmised that the inclusion of O containing species at the surface of the film resulted in charge trapping and scattering effects at the electrode/dielectric interface at high temperatures. Meddeb et al. [15] also posited that the mechanism dominating conduction through the material could potentially be changed and controlled using surface chemical modification. To this date and to the best of our knowledge, this hypothesis remains untested. In the present work, the current density vs electric field [$J(E)$] behavior of PI films measured in Meddeb et al. [15]. (https://doi.org/10.1016/j.cplett.2016.02.037) is analyzed using a series of theoretical frameworks that describe conduction through insulators and semiconductors to investigate the effect that O_2 plasma surface treatment has on high-field conduction in polyimides over a broad temperature range. This study will leverage further research that focuses on the role of dielectric/electrode interface in controlling conduction in PI and other organic dielectrics.

Analytical methods

Past research on PI has demonstrated the material's propensity to conduct via various charge transport mechanisms. Work by Diaham et al. [29] investigated conduction characteristics of thin (1.4 μm) PI films under high electric fields (in the range of 100 MV/m) and high temperatures (320–400 °C). In Diaham's work [29], analysis of pre-breakdown currents as a function of field and temperature suggests conduction at very high temperatures and fields preceding dielectric breakdown is a space-charge-dominated process. This result coincides well with results obtained by Kishi et al. [30] where pulsed electroacoustic measurements demonstrate hetero-space-charge formation increase as a function of field intensity and temperature prior to breakdown. Both of these studies involve either application of very high electric fields for long times (Kishi ~ 260 MV/m at $t > 10$ min [30]) or sample exposure to extremely high temperature (Diaham $T = 400$ °C [29]) to stress the material in the range of pre-dielectric breakdown. Space-charge measurements under less extreme conditions by laser intensity modulation method in 10 μm PI films for long timescales ($t \sim 30$ min) and moderate fields ranging 0.5–2 MV/m show charge accumulation within the samples dependent on electronic charge injection at the anode and cathode [31]. Given these results, the analysis in this manuscript will be carried out using a combination of theoretical frameworks that describe both bulk-dominated and interface-dominated processes which are reviewed in the following section.

Bulk-dominated conduction

Conduction through polymer dielectrics are typically analyzed using one of two theoretical frameworks: Poole–Frenkel (PF) or hopping [32]. The PF model for conduction describes field-enhanced thermal de-trapping of electrons or holes from impurity centers

distributed through the bulk of the material [33]. In the case of PI and other organics such as polytetrafluoroethylene (PTFE), this framework is typically considered because of the high density of impurity centers located within the bulk of the film arising from its partly amorphous structure [34]. The PF transport current is defined by Eq. (1):

$$J_{PF} = \sigma E e^{\frac{\beta_{PF} E^{\frac{1}{2}}}{kT}} e^{\frac{-\phi_{PF}}{kT}}, \quad (1)$$

where J_{PF} is the current density, σ is a constant related to charge, carrier density, and carrier mobility, E is the electric field, k is Boltzmann's constant, T is temperature, ϕ_{PF} is the trap barrier height at zero field, and β_{PF} is a constant. In Eq. (1), $\beta_{PF} = (q^3/\pi\varepsilon_o\varepsilon_r)^{1/2}$ where q is the elementary charge and is related to field-assisted barrier height lowering in the material and ε_r is the material's dielectric constant.

Hopping conduction theory is similar to PF theory in that it describes a conduction process occurring through the material's bulk. In hopping, the charge carrier undergoes a diffusion-based carrier-hopping process [32, 33, 35]. The mathematical framework that governs this process is presented in Eq. (2):

$$J_H = J_o e^{\frac{-\phi_H}{kT}} \sinh\left[\frac{qdE}{2kT}\right]. \quad (2)$$

In Eq. (2), J_o is a constant of the form $nfdq$ with n defined as a carrier density, f carrier vibration frequency, d the distance between trap sites termed the "hop distance," and q the elementary charge. The term ϕ_H is typically referred to as an activation energy or barrier height for the hopping conduction process [33, 36].

Interface-dominated conduction

In this work, we also consider the possibility of Schottky-type emission. Schottky theory assumes that conduction is dominated by charge emission through the dielectric/electrode interface. This framework is considered in the analysis of plasma-treated PI for two reasons: (1) The fact that plasma treatment is a surface modification process, and (2) the treatment's influence on conduction that has been observed at high temperatures [15]. The mathematical framework for Schottky emission is very similar to PF-type conduction and is presented in Eq. (3) below.

$$J = A^* T^2 e^{\frac{\beta_S E^{\frac{1}{2}}}{kT}} e^{\frac{-\phi_S}{kT}} \quad (3)$$

Equation (3) differs from (1) by the three main parameters A^*, ϕ_S, *and* β_S. The constant A^* is the Richardson constant and has the form $4\pi q m_e k^2/h^3$, with m_e being the mass of an electron and h is Plank's constant. ϕ_S is the Schottky barrier height defined by the difference between metal contact work function and electron affinity of the test material, and β_S is a constant related to field-assisted barrier height lowering. In Schottky, $\beta_S = (q^3/4\pi\varepsilon_o\varepsilon_r)^{1/2}$ and is slightly different than that of PF emission because it takes into account the image force potential associated with charge leaving the electrode during injection.

Results and analysis

Leakage current results

Kapton® PI samples, 13 μm thick, were obtained from Dupont. The PI and PPIDS sample sets consists of three untreated and plasma-treated samples (respectfully) electroded using 100-nm evaporated silver. During electrode evaporation, each sample set was exposed to high vacuum (10^{-6} Pa) for approximately 2 h. Electrodes were circular and 1 cm in diameter for each sample. The three samples labeled PPIDS are plasma-treated with O_2 on both sides of the film prior to electrodes deposition. The flow rate was held at 200 sccm, and the treatment power was 200 W that lasted 5 min/side. During plasma treatment, low vacuum was applied, stabilizing between 0.42 and 0.45 Pa. Details concerning specifics about PI surface chemical characterization as well as $J(E)$ data acquisition are present in the parent study and made available to the dedicated reader in Meddeb et al. [15]. (https://doi.org/10.1016/j.cplett.2016.02.037).

Current voltage measurements were performed using a Hewlett Packard 4140B pA meter that served as its own DC source connected to a Trek voltage amplifier model 10/10B-HS. Initial measurement of the charging current transients in PI was done at the lowest fields of measurement used in this study (8–23 MV/m) and at room temperature. Figure 1 shows charging current as a function of time. The lowest current measured was 40 pA (after a 100-s voltage hold time) with 8 MV/m applied, which is well above the minimum 1 pA that can be measured by the pA meter. Steady state in the measurement begins at 20 s indicated by a plateau in charging current. At higher temperature and fields, plateauing

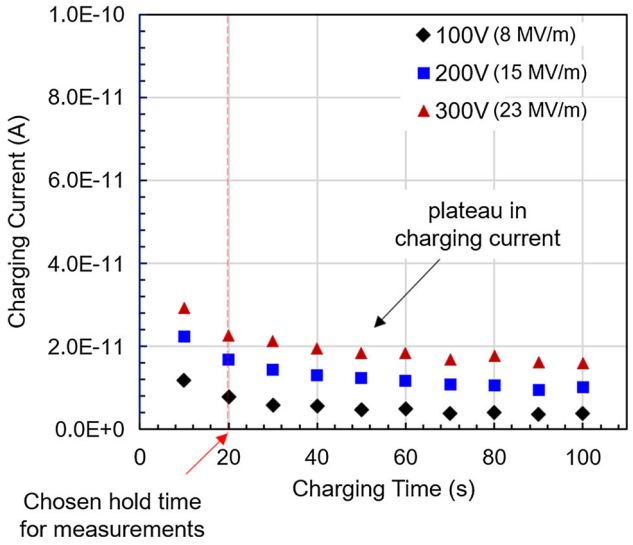

Figure 1 Charging current measured for PI as a function of charge time at room temperature.

in the current occurs at shorter times, making 20 s a reasonable hold time where a) steady state in the current is achieved and b) the chance for sample degradation at high fields and high temperatures is minimized.

A significant reduction in leakage current through PI was measured following O_2 plasma surface treatment in our previous study by Meddeb et al. [15] and is shown in Fig. 2. At low temperatures, the average current density of both the untreated PI and O_2 plasma-treated PPIDS data sets are within the same range. As temperature increases to 150 °C, the average current density for PI at 115 MV m^{-1} is 4.04×10^{-4} A m^{-2} which is an order of magnitude larger than the PPIDS measured to be 4.07×10^{-5} A m^{-2}. At all temperatures, there is less scatter in the data for plasma-treated samples relative to the untreated control set; however, this is especially true at high temperatures and electric fields. Due to the similarities in sample storage and processing between the PI and PPIDS sample sets, changes in current magnitude and scatter are linked back to a change in surface chemistry after the plasma treatment procedure: Increases in hydroxyl as well as carbonyl and carboxyl groups due to treatment are detailed in Meddeb et al. [15] and have also been reported by Inagaki et al. [37] to be present in Kapton® films post-oxygen plasma treatment.

The impact that plasma treatment has on the magnitude of leakage current through the film as a function of temperature and field can be seen from

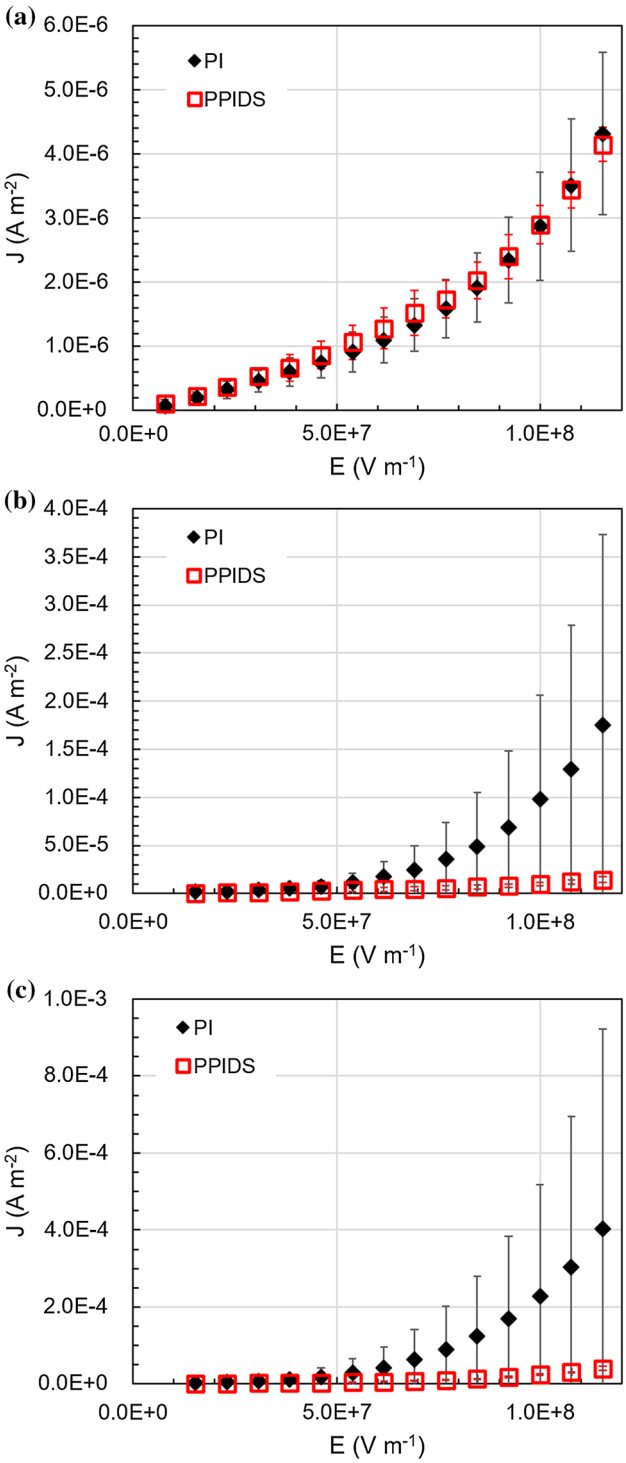

Figure 2 $J(E)$ data for untreated and O_2 plasma surface-treated PI at **a** 25 °C, **b** 100 °C, and **c** 150 °C. Applied voltage is held for 20 s (time required to obtain steady-state conduction) before current measurement at each field.

the data presented in Fig. 2; however, the exact mechanisms responsible for this reduction are not yet determined. It is important to seek out the exact

mechanisms by which plasma surface treatment limits conduction so that similar results can be exploited to decrease leakage currents and improve high-field and high-temperature performance of dielectric films. This requires quantitative analysis under a set of theoretical frameworks that describe high-field conduction through dielectrics. The following sections use the theoretical frameworks that describe bulk-dominated and interface-dominated conduction to quantify how plasma surface treatment achieves reduced leakage current and discuss its impact for future high-temperature capacitor development.

Data analysis

Modeling bulk conduction

Initially, PF theory is considered. The linearization of Eq. (1) leaves the following expression for conduction under PF framework:

$$\mathrm{Ln}\left(\frac{J_{\mathrm{PF}}}{E}\right) = \frac{\beta_{\mathrm{PF}}E^{1/2}}{kT} - \frac{\phi_{\mathrm{PF}}}{kT} + \mathrm{Ln}(\sigma) \tag{4}$$

The slope of linearized data can be directly related to β_{PF} at a single temperature T. Since $J(E)$ data were recorded isothermally at temperatures ranging between 25 and 175 °C, the permittivity of PI can be extracted directly from the slope of the PF plots using the expression for β_{PF} stated in "Bulk-dominated conduction" section. This procedure is done at each temperature by applying a linear regression fit to the data plotted in PF plot format (Ln(J/E) vs. $E^{1/2}$). The slope m of the regression function is then converted to permittivity using the following equation:

$$\epsilon_{\mathrm{r,PF}} = \left[\frac{(mkT)^2\pi\varepsilon_o}{q^3}\right]^{-1} \tag{5}$$

Treatment of the data in this manner produces $\varepsilon_{\mathrm{r,PF}}$ values that range between 500 and 20 depending on temperature. Considering that PI's accepted range in permittivity is between ~ 2.25 at high frequencies and ~ 3.15 at 1 kHz, it is concluded that PF theory inadequately describes the behavior of the material.[1]

[1] More information on PF analysis including treatment of data and calculated values of $\varepsilon_{\mathrm{r,PF}}$ are provided in the supporting supplemental document, section *1-i*.

Past work done on PI by Sawa et al. [38] and Sacher [39] suggest that room-temperature conduction through the material is a result of proton hopping originating from carboxyl groups in unreacted polyamic acid (PAA) within the bulk of the material. Hopping conduction is described using Eq. (2) and is more complex than Eqs. (1) and (3). This equation cannot be linearized to calculate fit parameters J_o, ϕ_H, and d. Instead, fitting is performed using the statistical software RStudio where a nonlinear regression technique optimizes the parameters J_o and d to minimize the sum of squares between Eq. (2) and raw data.

In hopping conduction theory, the value of ϕ_H is taken as low field activation energy. In this study, low field activation energy is estimated using the following Arrhenius-type equation for conduction

$$I = I_o e^{\frac{-\phi_H}{kT}}, \tag{6}$$

where I is measured current, and I_0 is a constant associated with conduction as ϕ_H approaches 0. Figure 2 demonstrates how surface chemical modification reduces leakage current, potentially impacting the conduction mechanism at high temperatures and fields. For this reason, the PI set is used to extract low field activation energy to exclude effects introduced by plasma treatment. $I(V)$ data for the PI set are plotted as a function of Ln(I) versus T^{-1} and presented in Fig. 3.

Measurements taken at 100 V at each temperature were used for low field currents. The data are described well using the Arrhenius relation in Eq. (6) and returns an activation energy of 0.25 eV, which is within range reported in studies where PI was processed by solution casting and vapor deposition under AC and DC field conditions [36, 40]. Similarly, $\phi_H < 1.0$ eV is indicative of electronic-based conduction in the film, implying electrons may play a role as charge carriers during DC conduction in the film [40]. This result can be related back to work done by Ito et al. [36], Sawa et al. [38], and Sacher [39] where the conduction through PI films was found to be dependent on proton hopping stemming from the carboxyl group presence due to unreacted PAA. In the current study, PI films are obtained from Dupont and are of high quality. Although the complete absence of proton conduction from carboxyl entities is not guaranteed, the quality of the films suggests limited proton conduction resulting from unreacted

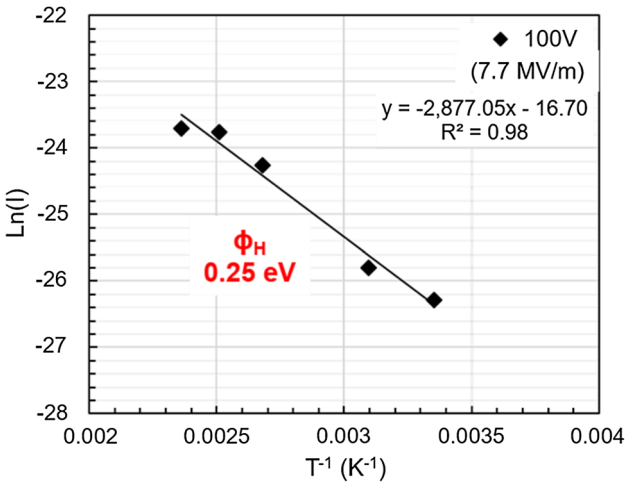

Figure 3 Arrhenius plot for Pure P1 over the temperature range 25–150 °C. Activation energy is extracted from linearization of Eq. (6) and the slope of the linear fit function.

PAA compared to PI films studied by Sacher [39]. This analysis coincides well with work done by Tu and Kao [41], where C-V experiments performed on 100% imidized PI suggest conduction is dominated by an electron transport process, potentially occurring via hopping along acceptor states both along the polymer chain's backbone and between adjacent chains.

A combination of physical arguments as well as statistical analysis was used to assess the validity of the hopping model to explain the J(E) behavior. Due to the form of the function used to fit J(E) data, calculation of P values should not be implemented to determine parameter estimate significance. Nonlinear models do not have a well-defined relationship between parameter (in this case d and Jo) and predictor variables (applied field E), which inhibits the creation of a single hypothesis test that can represent all nonlinear models. A more appropriate method to determine parameter significance for our purposes would be computation of a confidence interval for each parameter estimate. Unfortunately, the distributions of fit parameters describing the sample sets are unknown and difficult to extract from measurements given the sample size N = 3 in each sample set. To estimate a distribution for the parameters, bootstrap statistics are employed where variation of fit parameters that describe the data set can be estimated by sampling with replacement. This method yields a confidence interval for Jo and d that reflects variation among the samples comprising PI and PPIDS sample sets.[2,3]

Physical arguments concerning the model's validity begin by examining the hop distance. Values of d are first considered to assess how well the hopping model describes sample behavior and are plotted in Fig. 4 for both sample sets as a function of temperature. Hop distance estimated for both sample sets ranges between ~ 10 and 30 Å, which is within the range of hop distances reported in the literature for PI and also BOPP [11, 36, 42, 43]. At room temperature, d is estimated to be approximately 12 Å, which is quite close to the length of the chemical repeat unit of PI (~ 15 Å measured by X-ray diffraction in Ito et al. [36]) which suggests hopping conduction propagates in the polymer chain direction through the material. At higher temperatures, the hop distance increases in both sample sets: 25 Å in PI at 75 °C and 24 Å at 125 °C in PPIDS. This exceeds the chemical repeat unit for the material and may reflect a transition from intrachain to interchain charge carrier hopping at higher temperatures.

J_o is also analyzed across the measurement's temperature range. Using the relation $J_o = nfqd$, a nf (product of carrier density and vibration frequency) can be calculated from fit estimates. The product nf ranges from 1.6×10^{25} to 4.4×10^{25} m^{-3} s^{-1} in PI between 25–75 °C, and from 5.6×10^{24} and 8.0×10^{25} m^{-3} s^{-1} in the PPIDS set between 25 and 125 °C. These ranges are compared to previous work done by Ito et al. [36] that focuses on the effect of curing vapor-deposited PI films. Films undergoing 4 h of curing returned nf values after fitting on the order of 1×10^{21} m^{-3} s^{-1} while uncured films returned 1×10^{35} m^{-3} s^{-1}. The films used in this study produce a value of nf within the range reported by Ito et al. Small differences can be expected considering the difference in sample preparation, as well as fitting procedures used: Ito et al. [36] obtains higher activation energy of 0.34 eV and uses a series of low and high-field approximations on Eq. (2) in fitting.

[2] A more detailed outline of the bootstrap statistical approach can be found in the supporting supplemental document, section *1-ii, a* and *b*. Content found in this manuscript is focused on statistical interpretation only.

[3] Annotated RStudio script used for fitting and bootstrap analysis is found in section *2-i* of the supporting supplemental document.

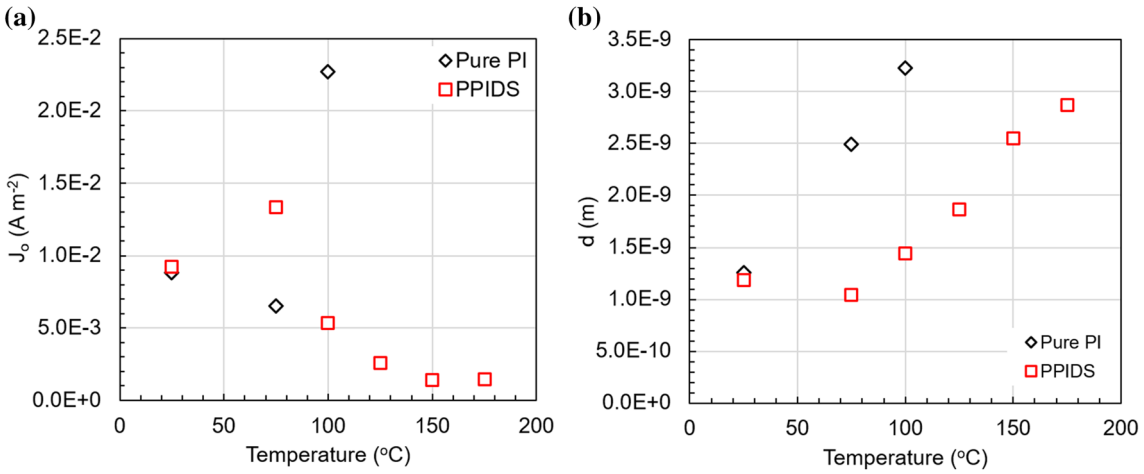

Figure 4 Hopping parameters J_o and d estimated using the bootstrapping statistical approach.

Table 1 Parameter fit values and confidence intervals at each temperature for untreated PI sample set

Temperature (°C)	25	75	100	125	150	175
$J_{o_{estimated}}$	6.98×10^{-4}	7.36×10^{-4}	2.56×10^{-3}	–	–	–
2.5% CI	3.66×10^{-4}	1.03×10^{-5}	1.67×10^{-9}	–	–	–
97.5% CI	1.16×10^{-3}	2.23×10^{-3}	8.25×10^{-3}	–	–	–
$d_{estimated}$	1.26×10^{-9}	2.50×10^{-9}	3.18×10^{-9}	–	–	–
2.5% CI	9.52×10^{-10}	1.38×10^{-9}	1.03×10^{-9}	–	–	–
97.5% CI	1.60×10^{-9}	4.66×10^{-9}	1.04×10^{-8}	–	–	–

No values for J_o or d are provided because of the program's inability to fit the data using Eq. (2)

Statistical interpretation of the fit results was used to comment on the behavior of the sample set as a function of temperature. At 25 °C, there is very little change in the estimated values of either fit parameters between sample sets. This is an expected outcome considering similarity in behavior between PI and PPIDS sample sets at low temperature reported in Fig. 2. It is also noted that the estimates of d and J_o are centered within their respective confidence intervals computed by bootstrapping which are presented in Table 1 for PI. This implies that the estimated parameters follow a symmetric distribution, which is most likely caused by the samples within the data sets behaving similar to one another as a function of electric field. As temperature is increased to 100 °C, a significant separation in the values of J_o and d estimated from PI and PPIDS sets occurs. Both parameters for the PI set exceed values computed for PPIDS. Greater change can be noted in the 95% confidence intervals for both fit parameters in PI. At 100 °C, the confidence interval pertaining to d ranges a full order of magnitude. Similarly, the estimated value of d is no longer centered within the confidence interval, indicating an asymmetric distribution for hop distance. A similar outcome exists for J_o displaying an asymmetric distribution with confidence interval ranging seven orders of magnitude at 100 °C, indicating a major variation between the samples comprising the PI data set. These outcomes of fitting d and J_o at high temperature diminish the significance of their estimated values, indicating a poor fit to the data. Unlike PI, the PPIDS sample set does not show a pronounced change in fit parameters within 25–100 °C. The confidence intervals for both fit parameters are also significantly tighter and do not display asymmetry, as shown in Table 2, suggesting that samples within the set behaving quite similarly as a function of field within this temperature range, coinciding nicely with small standard deviations calculated for PPIDS $J(E)$ data in Fig. 2.[4]

[4] Histograms of parameter estimates from which confidence intervals are derived are presented in the supporting supplemental document, section *3-i-a*. Raw data is plotted with superimposed nonlinear fits in section *3-i-b*.

Table 2 Parameter fit values and confidence intervals at each temperature for the plasma-treated PPIDS sample set

Temperature (°C)	25	75	100	125	150	175
$J_{o_{estimated}}$	7.36×10^{-4}	1.53×10^{-3}	7.12×10^{-4}	3.94×10^{-4}	2.34×10^{-4}	2.70×10^{-4}
2.5% CI	6.17×10^{-4}	9.09×10^{-4}	4.24×10^{-4}	2.45×10^{-4}	1.61×10^{-4}	1.84×10^{-4}
97.5% CI	8.70×10^{-4}	2.45×10^{-3}	1.13×10^{-3}	5.74×10^{-4}	3.03×10^{-4}	3.58×10^{-4}
$d_{estimated}$	1.19×10^{-9}	1.04×10^{-9}	1.44×10^{-9}	1.86×10^{-9}	2.55×10^{-9}	2.87×10^{-9}
2.5% CI	1.10×10^{-9}	7.59×10^{-10}	1.11×10^{-9}	1.57×10^{-9}	2.34×10^{-9}	2.64×10^{-9}
97.5% CI	1.27×10^{-9}	1.32×10^{-9}	1.75×10^{-9}	2.18×10^{-9}	2.84×10^{-9}	3.18×10^{-9}

Interface-dominated conduction

Schottky analysis was performed in a similar manner to PF by the linearization of Eq. (3):

$$\mathrm{Ln}(J_S) = \frac{\beta_S E^{1/2}}{kT} - \frac{\phi_S}{kT} + \mathrm{Ln}\left(A^* T^2\right). \tag{7}$$

In Eq. (7), the $J(E)$ data are plotted in a Shottky plot ($\mathrm{Ln}(J_s)$ vs. $E^{1/2}$) where linear fit slope can be used to calculate material permittivity using the form of β_S discussed in "Interface-dominated conduction" section. The data from Fig. 2 are transformed into Schottky plot format and shown in Fig. 5 along with their respective linear fit functions.

Both PI and PPIDS data sets behave similarly at 25 °C, which is expected given previous observations, as shown in Fig. 2. At 100 °C, a change in the sample sets' behaviors occurs where the slope of linear fit corresponding to PI becomes steeper compared to that of PPIDS. As temperature is increased to 150 °C, the difference between these slopes still exists; however, it is less dramatic. This implies that the value of permittivity calculated using Schottky theory will change depending on both temperature and sample processing condition. Calculation of permittivity under Schottky formalism is done via the following equation:

$$\epsilon_{r,S} = \left[\frac{(mkT)^2 4\pi\varepsilon_o}{q^3}\right]^{-1} \tag{8}$$

Permittivity values calculated for each sample group as a function of measurement temperature are shown in Fig. 6. At low temperatures, Schottky theory produces permittivity values within the range of 18 to 4 for PI, indicating that this model inadequately describes conduction through the material. This outcome coincides well with modeling performed using hopping theory in Modeling bulk conduction that confirms that low-temperature conduction is better described by a bulk-dominated process. At elevated temperatures, starting at 100 °C, the PI sample set undergoes a transition in behavior and returns a calculated permittivity that lies within the range considered acceptable for PI. The value of permittivity calculated using Schottky theory remains within the range of expected permittivities for the material (determined by the high-frequency permittivity given by refractive index squared (n^2) and ε_r measured at 1 kHz) up until 150 °C indicating that high-temperature conduction is no longer dominated by hopping but rather injection through the electrode/dielectric interface.

Unlike the PI, PPIDS samples do not display Schottky-type behavior at low and moderate temperatures. In fact, Schottky theory does not return a permittivity within the expected range of PI until 150 °C and is located at the upper limit of acceptable permittivity for polyimide. At 175 °C, the calculated permittivity for the PPIDS films are well within the expected range for PI, displaying a value similar to untreated PI at 100 °C. This demonstrates that high-field conduction in plasma-treated polyimide can be described by a Schottky-dominated process only after the film is exposed to 75 °C higher temperature than untreated PI. This result is in good agreement with the results obtained from "Modeling bulk conduction" section that yielded good fits using hopping theory spanning the entire temperature range for the PPIDS set.

Discussion and conclusions

Plasma surface treatment using a mixture of oxygen and helium gas demonstrates the ability to chemically alter the surface environment of PI, changing both wetting and electrical properties of the film. Results obtained from XPS measurements on plasma-

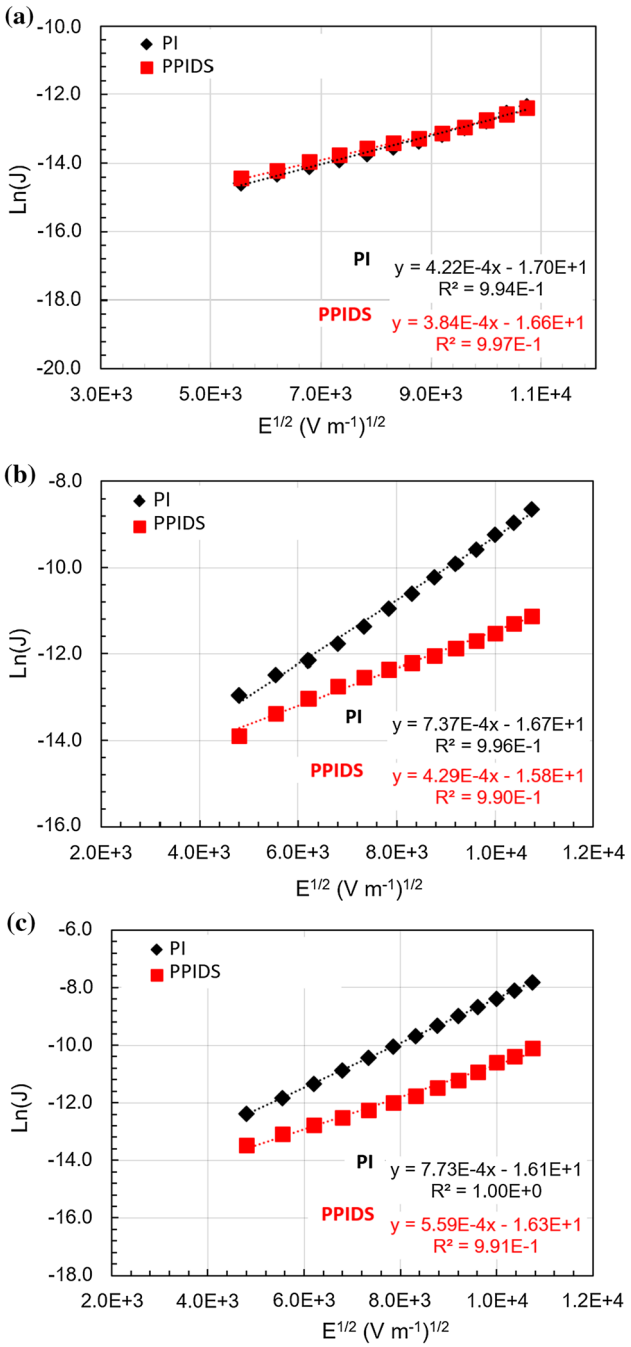

Figure 5 $J(E)$ data from Fig. 2 transformed into Schottky plot format. Again, measurements were taken at **a** 25 °C, **b** 100 °C and **c** 150 °C. Here slope of linear fit corresponds to β_s/kT in Eq. (7).

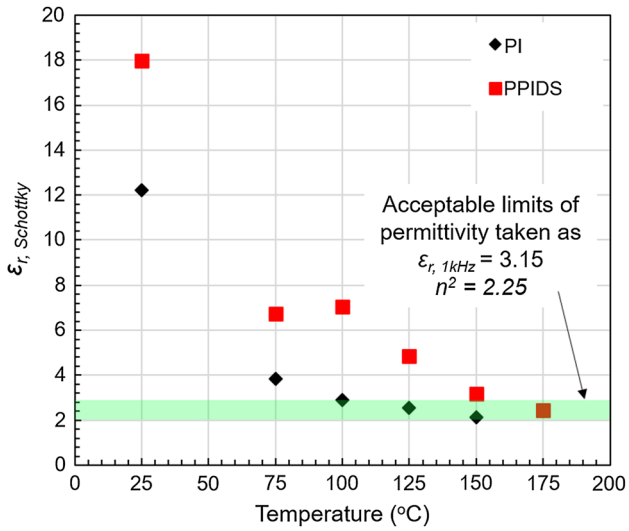

Figure 6 Permittivity values calculated from linear fits from Schottky plots between 25 and 175 °C. A shaded region is marked indicating the range between high-frequency permittivity (n^2) and permittivity measured between 100 Hz and 100 kHz.

treated PI from the previous study by Meddeb et al. [15] indicate the increase of hydroxyl groups and suggest the formation of added carbonyl and carboxyl moieties to the surface of the films.

In our previous study by Meddeb et al. [15], the addition of these chemical moieties is surmised to result in the high-field conduction suppression, suggesting that their presence serves to trap or scatter charges at the interface. In this present work, it is shown that low-temperature conduction through untreated PI and plasma-treated PI is dominated by a hopping-type mechanism, governed by the diffusion of charge carriers through the bulk of the film. PI is shown to diverge from this model at 100 °C, exhibiting conduction that is well described by Schottky theory, indicating charge injection at the electrode/dielectric interface. Calculation of the activation energy in the low field regime indicates the activation energy for DC conduction through an untreated film is 0.25 eV implying the presence of electronic charge carriers. This result strengthens the outcome of high-temperature conduction modeling, suggesting that electronic injection dominates leakage current through the material under the combination of sufficiently high electric field and temperatures.

Plasma treatment increases the hopping-Schottky conduction transition temperature from 100 to 175 °C. This result indicates that the combination of hydroxyl, carbonyl, and carboxyl groups grafted by plasma treatment could be preventing charge injection at the interface. Previous mention of the conduction at high temperature dominated by electronic injection at the electrode/dielectric interface coincides well with this theory: Electronegative-oxygen-containing moieties create electron-trapping centers

at the interface and limit current injection at high temperatures. This finding correlates well with past research that demonstrates conduction is electronically dominated [41, 44], indicating that the high-temperature performance of PI can be improved by simple surface chemical modification using O_2 to suppress charge injection of electronic carriers. Similarly, plasma treatment can potentially limit the formation of electronic space charges in dielectrics in the context of work done by Locatelli et al. [31], thereby reducing field enhancements at the electrode/dielectric interface. Future research concerning PI's applicability for high-temperature dielectrics should emphasize the role of the electrode/dielectric interface and its potential to be used in tailoring electrical properties of the material. The outcomes from theoretical analysis of data are used to provide further insight into how surface chemistry may be used to tailor high-field leakage current in PI, and other materials. Suppressing leakage current by plasma surface treatment will potentially lead to improved capacitor performance by limiting joule heating, suppressing electronic space-charge development under high fields, and extending the operable temperature range of dielectric materials for power applications.

Acknowledgements

The authors of this publication would like to acknowledge the support of the National Science Foundation as part of the Center for Dielectrics and Piezoelectrics under Grant Nos. IIP-1361571 and IIP-1361503. We also would like to acknowledge Adam Walder for his expertise in RStudio script writing and input on statistical analysis of parameter estimates from nonlinear regression. Adam is a Ph.D. student in the department of statistics as part of the Eberly College of Science at Penn State.

Compliance with ethical standards

Conflict of interest The authors declare that they have no conflict of interest.

Electronic supplementary material: The online version of this article (https://doi.org/10.1007/s10853-019-03574-w) contains supplementary material, which is available to authorized users.

References

[1] Laihonen SJ, Gafvert U, Schutte T, Gedde UW (2007) DC breakdown strength of polypropylene films: area dependence and statistical behavior. IEEE Trans Dielectr Electr Insul 14(2):275–286

[2] Zhu J (2018) Theory of Ragone plots for electrostatic energy storage. B.S. thesis in engineering science and mechanics

[3] Zhu L, Wang Q (2012) Novel ferroelectric polymers for high energy density. Macromolecules 45(7):2937–2954

[4] Zhang X, Shen Y, Shen Z, Jiang J, Chen L, Nan C-W (2016) Acheiving high energy density in PVDF-based polymer blends: suppression of early polarization saturation and enhancement of breakdown strength. Appl Mater Interfaces 8(40):27236–27242

[5] Mackey M, Hiltner A, Baer E, Flandin L, Wolak MA, Shirk JS (2009) Enhanced breakdown strength of multilayered films fabricated by forced assembly microlayer coextrusion. J Phys D Appl Phys 42(17):1–11

[6] Christen T, Carlen MW (2000) Theory of Ragone plots. J Power Sources 91:210–216

[7] Huan TD, Boggs S, Teyssedre G, Laurent C, Cakmak M, Kumar S, Ramprasad R (2016) Advanced polymeric dielectrics for high energy density applications. Prog Mater Sci 83:236–269

[8] Gregorio R Jr, Ueno EM (1999) Effect of crystalline phase, orientation and temperature on dielectric properties of poly(vinylidene fluoride) (PVDF). J Mater Sci 34:4489–4500. https://doi.org/10.1023/A:1004689205706

[9] Vecchio MA, Meddeb AB, Lanagan MT, Ounaies Z, Shallenberger JR (2018) Plasma surface modification of P(VDF–TrFE): influence of surface chemistry and structure on electronic charge injection. J Appl Phys 124(11):114102

[10] Umemura T, Akiyama K, Couderc D (1986) Morphology and electrical properties of biaxially-oriented polypropylene films. IEEE Trans Electr Insul EI-21(2):137–144

[11] Ho J, Jow RT (2012) HIgh field conduction in piaxially oriented polypropylene at elevated temperature. IEEE Trans Dielectr Electr Insul 19(3):990–995

[12] O'Dwyer JJ (1982) Breakdown in solid dielectrics. In: Conference on electrical insulation and dielectric phenomena—annual report, Amherst, MA, USA

[13] Johnson RW, Evans JL, Jacobson P, Thompson R (2002) High-temperature automotive electronics. In: Proceedings of international conference for advanced packaging and systems, Reno, Nevada

[14] Johnson RW (2004) The changing automotive environment: high-temperature electronics. IEEE Trans Electron Packag Manuf 27(3):164–176

[15] Meddeb AB, Ounaies Z, Lanagan MT (2016) Enhancement of electrical properties of polyimide films by plasma treatment. Chem Phys Lett 649:111–114. https://doi.org/10.1016/j.cplett.2016.02.037

[16] Hergenrother PM, Watson KA, Smith JG Jr, Connell JW, Yokota R (2002) Polyimides from 2,3,3′,4′-biphenyltetracarboxylic dianhydride and aromatic diamines. Polymer 43(19):5077–5093

[17] Hergenrother PM (2003) The use, design, synthesis, and properties of high performance/high temperature polymers: an overview. High Perform Polym 15:3–45

[18] Khazaka R, Locatelli ML, Diaham S, Bidan P, Dupuy L, Grosset G (2013) Broadband dielectric spectroscopy of BPDA/ODA polyimide films. J Phys D Appl Phys 46:065501

[19] Egitto FD, Emmi F, Horwath RS (1985) Plasma etching of organic materials. I. Polyimide in O_2–CF_4. J Vac Sci Technol B Microelectron Process Phenom 3(3):893–904

[20] Yaghoubi H, Taghavinia N (2011) Surface chemistry of atmospheric plasma modified polycarbonate substrates. Appl Surf Sci 257(23):9836–9839

[21] Kaminska A, Kaczmarek H, Kowalonek J (2002) The influence of side groups and polarity of polymers on the kind and effectiveness of their surface modification by air plasma action. Eur Polym J 38(9):1915–1919

[22] Yang C, Li X-M, Ilron J, Kong D-F, Yin Y, Oren Y, Linder C, He T (2014) CF4 plasma-modified superhydrophobic PVDF membranes for direct contact membrane distillation. J Membr Sci 456:155–161

[23] Park S-J, Lee H-Y (2005) Effect of atmospheric-pressure plasma on adhesion characteristics of polyimide film. J Colloid Interface Sci 285(1):267–272

[24] Ginn BT, Steinbock O (2003) Polymer surface modification using microwave-oven-generated plasma. Langmuir 19(19):8117–8118

[25] Shenton MJ, Lovell-Hoare MC, Stevens GC (2001) Adhesion enhancement of polymer surfaces by atmospheric plasma treatment. J Phys D Appl Phys 34(18):2754–2760

[26] Li C-Y, Liao Y-C (2016) Adhesive stretchable printed conductive thin film patterns on PDMS surface with atmospheric plasma treatment. ACS Appl Mater Interfaces 8(18):11868–11874

[27] Mammone RJ, Binder M (1992) Increased breakdown strengths of polypropylene films melt-extruded from plasma-treated resin. J Appl Polym Sci 46(9):1531–1534

[28] Mammone RJ, Binder M (1992) Effects of CF_4/O_2 gas plasma power/exposure time on dielectric properties and breakdown voltages of PVDF films. J Appl Polym Sci 46(9):1531–1534

[29] Diaham S, Locatelli M-L (2012) Space-charge-limited currents in polyimide films. Appl Phys Lett 101:242905. https://doi.org/10.1063/1.4771602

[30] Kishi Y, Hashimoto T, Miyake H, Tanaka Y, Takada T (2009) Breakdown and space charge formation in polyimide film Breakdown and space charge formation in polyimide film. J Phys Conf Ser 183:012005

[31] Locatelli M-L, Pham CD, Diaham S, Berquez L, Marty-Dessus D, Teyssedre G (2017) Space charge formation in polyimide films and polyimide/SiO_2 double-layer measured by LIMM. IEEE Trans Dielectr Electr Insul 24(2):1220–1228

[32] Das-Gupta D (1997) Conduction mechanisms and high-field effects in synthetic insulating polymers. IEEE Trans Dielectr Electr Insul 4(2):149–156

[33] Kao KC (2004) Dielectric phenomena in solids. Elsevier, Amsterdam

[34] Vollmann W, Poll H-U (1975) Electrical conduction in thin polymer fluorocarbon films. Thin Solid Films 26(2):201–211

[35] Das Gupta DK, Noon T (1975) Phototransient spectral shifts in polyethylene with high fields. J Phys D Appl Phys 8:1333–1340

[36] Ito Y, Hikita M, Kimura T (1990) Effect of degree of imidization in polyimide thin films prepared by vapor deposition polymerization on the electrical conduction. Jpn J Appl Phys 29(6):1128–1131

[37] Inagaki N, Tasaka S, Hibi K (1992) Surface modification of Kapton film by plasma treatments. J Polym Sci, Part A: Polym Chem 30:1425–1431

[38] Sawa G, Nakamura S, Iida K, Ieda M (1980) Electrical conduction of polypyromellitimide films at temperatures of 120–180 C. Jpn J Appl Phys 19:453

[39] Sacher E (1979) Dielectric Properties of Polyimide Film. II. DC Properties. IEEE Trans Electr Insul EI-14(2):85–93

[40] Muruganand S, Narayandass S, Mangalaraj D, Vijayan TM (2001) Dielectric and conduction properties of pure polyimide films. Polym Int 50:1089–1094

[41] Tu NR, Kao KC (1999) High-field electrical conduction in polyimide films. J Appl Phys 85(10):7267–7275

[42] Ikezaki K, Kaneko T, Sakakibara T (1981) Effect of crystallinity on electrical conduction in polypropylene. Jpn J Appl Phys 20(3):609–615

[43] Raju GG, Shaikh R, Haq SU (2008) Electrical conduction processes in polyimide films-I. IEEE Trans Dielectr Electr Insul 15(3):663–670

[44] Sessler GM, Hahn B, Yoon DY (1986) Electrical conduction in polyimide films. J Appl Phys 60(1):318–326